

## Trace Metals Optimization in Ceria Abrasive for Material Removal Rate Enhancement during ILD CMP

To cite this article: Cheolmin Shin *et al* 2017 *ECS J. Solid State Sci. Technol.* **6** P687

View the [article online](#) for updates and enhancements.

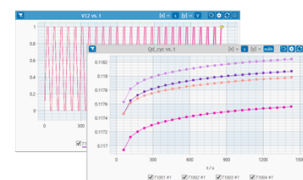
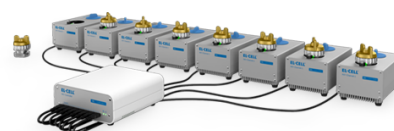
### You may also like

- [Redox Potential Measurements of Cr\(II\)/Cr Ni\(II\)/Ni and Mg\(II\)/Mg in Molten  \$\text{MgCl}\_2\text{-KCl-NaCl}\$  Mixture](#)  
Mingyang Zhang, Jianbang Ge, Taiqi Yin et al.
- [Unconventional ferrimagnetism and enhanced magnetic ordering temperature in monolayer  \$\text{CrCl}\_3\$  by introducing O impurities and Cl vacancies](#)  
Dario Mastroiolo, Jing Wang, Gianni Profeta et al.
- [Enhancement of electrical and photo-electrical properties of P3HT- \$\text{CrCl}\_3\$  thin films for photo sensing applications](#)  
Ali Mahdi and Furat A Al-Saymari

## PAT-Tester-x-8 Potentiostat: Modular Solution for Electrochemical Testing!

**EL-CELL<sup>®</sup>**  
electrochemical test equipment

- ✓ **Flexible Setup with up to 8 Independent Test Channels!**  
Each with a fully equipped Potentiostat, Galvanostat and EIS!
- ✓ **Perfect Choice for Small-Scale and Special Purpose Testing!**  
Suited for all 3-electrode, optical, dilatometry or force test cells from EL-CELL.
- ✓ **Complete Solution with Extensive Software!**  
Plan, conduct and analyze experiments with EL-Software.
- ✓ **Small Footprint, Easy to Setup and Operate!**  
Usable inside a glove box. Full multi-user, multi-device control via LAN.



Contact us:

☎ +49 40 79012-734

✉ [sales@el-cell.com](mailto:sales@el-cell.com)

🌐 [www.el-cell.com](http://www.el-cell.com)





## Trace Metals Optimization in Ceria Abrasive for Material Removal Rate Enhancement during ILD CMP

Cheolmin Shin,<sup>a</sup> Jinhak Choi,<sup>a</sup> Hojoong Kim,<sup>b</sup> Atul Kulkarni,<sup>c</sup> Donggeon Kwak,<sup>a</sup> Eungchul Kim,<sup>a</sup> and Taesung Kim<sup>a,z</sup>

<sup>a</sup>School of Mechanical Engineering, Sungkyunkwan University, Suwon, Gyeonggi Do 440-746, South Korea

<sup>b</sup>Cleaning/CMP Technology Team, Memory Business, Samsung Electronics, Banwol-dong, Hwasung-si, Gyeonggi-do, 445-701, South Korea

<sup>c</sup>Symbiosis Institute of Technology (SIT), Symbiosis International University (SIU), Lavale, Pune-41215, India

Ceria abrasive has been widely used in chemical mechanical planarization (CMP) to achieve a high material removal rate. To achieve optimum CMP performance,  $\text{Ce}^{3+}$  ions need to be generated on the ceria particle surface so they can react with  $\text{SiO}_2$ . Based on the redox reaction, trace metals can be good candidates for forming the required ions. In this study,  $\text{FeCl}_2$  and  $\text{CrCl}_2$  trace metals with ceria were evaluated in terms of their CMP performance and effectiveness. The role of oxygen vacancies formed on the ceria surface using trace metals was experimentally investigated. Compared to  $\text{FeCl}_2$ ,  $\text{CrCl}_2$  exhibits better CMP performance. We observed that with the addition of  $\text{CrCl}_2$  trace metals in the ceria abrasive, the removal rate of  $\text{SiO}_2$  was enhanced by 1.3 times that of only ceria abrasive. Further, in the presence of  $\text{CrCl}_2$ , the  $\text{SiO}_2$  wafer surface roughness was reduced from 0.473 nm to 0.390 nm.  
© 2017 The Electrochemical Society. [DOI: 10.1149/2.0241709jss] All rights reserved.

Manuscript submitted June 13, 2017; revised manuscript received July 25, 2017. Published September 28, 2017.

Chemical mechanical planarization (CMP) has been widely used in the microfabrication industry.<sup>1,2</sup> The material removal rate (MRR) is highly important in CMP to reduce the cost of consumables such as pads, slurries, and conditioners, along with improvisation in the production yield.<sup>3–5</sup> For interlayer dielectric (ILD) CMP, the use of ceria-abrasive-based slurries is becoming more prominent because they provide superior CMP performances, including high selectivity, high removal rate, and high planarization efficiency.<sup>6,7</sup> Since ceria-abrasive-based slurries are expensive, their functionality performance needs to be improved via the addition of other materials into the slurries.

99.99%, Sigma-Aldrich Inc., USA), were added in 1 wt. % ceria abrasive at concentrations of 10, 50, 100, 500 and 1000 ppm. The suspensions were adjusted to all have a pH of 10 using KOH; this is because the MRR depends only on the pH and ceria reactivity.<sup>12</sup>

**Chemical mechanical planarization test.**—A  $\text{SiO}_2$  wafer (Semiroad Co., South Korea) was prepared and polished (CP-4, Bruker, USA) for use as the substrate with a size of 40 mm × 40 mm. The polishing was carried out for 2 minutes. The  $\text{SiO}_2$  thickness was measured using a reflectometer (ST4000-DLX, K-MAC, South Korea) to calculate the MRR. The MRR was calculated as below equation,

$$\text{MRR} = \frac{\text{film thickness after polishing } (\text{\AA}) - \text{film thickness before polishing } (\text{\AA})}{\text{CMP process time (minutes)}} \quad [1]$$

To improve the chemical interaction between ceria abrasive and dielectrics using mainly  $\text{SiO}_2$ , it is necessary to create oxygen vacancies on the ceria abrasive surface.<sup>7,8</sup> To achieve this, several methods have been reported, including the mixture of different slurries, surfactant treatment of the slurries, and nano-composites of the ceria.<sup>9–11</sup> Among the various materials typically used, trace metals are well known for their high redox potential and surface energy, which can improve the reactivity of the ceria abrasive with a dielectric  $\text{SiO}_2$  wafer. Hence, there is a need to evaluate the effects of trace metals in ceria-abrasive-based slurries for improved MRR during CMP, which has not yet been explored in detail.

In the present work, an experimental investigation was carried out to determine the effects of trace metals on both ceria abrasive particle surfaces and their interaction with  $\text{SiO}_2$  wafers. The interaction between ceria abrasive and trace metals ( $\text{FeCl}_2$  and  $\text{CrCl}_2$ ) was evaluated by measuring the zeta potential and absorption spectra, as well as imaging using scanning electron microscopy (SEM). The CMP performance and wafer surface roughness were evaluated by estimating the MRR and by using atomic force microscopy (AFM), respectively.

### Experimental

**Materials.**—Commercially available calcined ceria abrasive slurry (KCS1300MS, KCTech Co., South Korea) was used in this experiment. Two different trace metals,  $\text{FeCl}_2$  and  $\text{CrCl}_2$  (anhydrous,

To minimize the chemical reaction by using other cleaning solutions, the  $\text{SiO}_2$  wafer was rinsed using only DI water after CMP. The details of the experimental procedure for the CMP process used in this study are presented in Table S1.

**Characterization.**—To analyze the dispersion stability behavior of the ceria abrasive in slurries, particle size distribution measurements were obtained using the scanning mobility particle sizer system (SMPS, TSI, USA). The electrokinetic behavior of the ceria abrasive was characterized using a zeta potential analyzer (Zetasizer Nano ZS, Malvern, England) at pH 10, and scanning electron microscopy (SEM, JEOL, Japan) was used to investigate particle agglomeration.

Ultraviolet-visible spectroscopy (Cary 5000, Varian, Australia) was employed to obtain the adsorption spectra of ceria abrasive for different trace metals and concentrations at room temperature. AFM images (Innova, Bruker, USA) of the surface for a  $2 \mu\text{m} \times 2 \mu\text{m}$  area were obtained using the tapping mode. To analyze the composition of the  $\text{SiO}_2$  wafer after the CMP process, the surface sputtering method was applied using secondary ion mass spectrometry (SIMS, TOF-SIMS-5, ION-TOF, Germany). The  $40 \times 40 \mu\text{m}^2$  area was measured and the positive method was used with 25 keV and 1.000 pA.

### Results and Discussion

Ceria abrasive with different concentrations of  $\text{FeCl}_2$  and  $\text{CrCl}_2$  was prepared as depicted in Figure S1. To maintain the pH at 10, KOH solution was added. Interestingly, it was observed that the ceria abrasive solution become transparent for  $\text{FeCl}_2$  at 1000 ppm and for

<sup>z</sup>E-mail: tkim@skku.edu

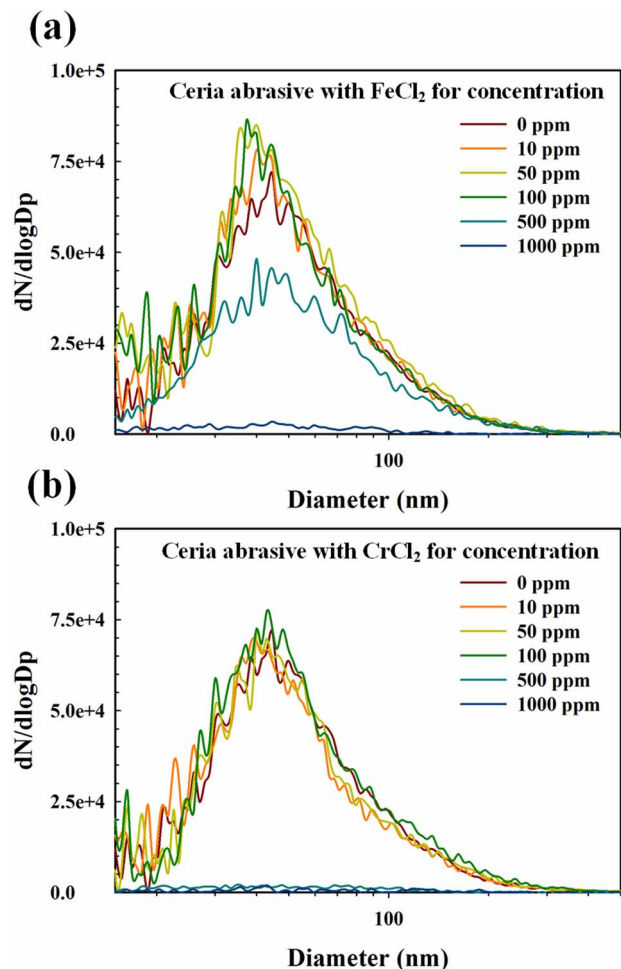


**Figure 1.** The particle size distribution of ceria abrasive with (a) FeCl<sub>2</sub> and (b) CrCl<sub>2</sub> (0, 10, 50, 100, 500, and 1000 ppm).

CrCl<sub>2</sub> at 500 and 1000 ppm. Further, the particle size distributions of these prepared ceria abrasives were evaluated as shown in Figure 1. It can be seen that the mode particle size of ceria abrasive without trace metals was 49.6 nm and there was no noticeable change in the particle mode size of the ceria abrasives with FeCl<sub>2</sub> and CrCl<sub>2</sub> up to 100 ppm, nor was there any change in particle number concentration; for the concentrations above 100 ppm however, the number of particles was found to be drastically decreased. A possible cause of this is the reaction of trace metals with hydroxyl groups (-OH) of the base solution, which may result in various salts such as Fe(OH)<sub>3</sub> or Cr(OH)<sub>3</sub>. We attempted to measure the agglomerated ceria abrasive particle number concentration, however we could not measure particle sizes above 300 nm due to limitations of the SMPS used in this study.<sup>13</sup> The electrokinetic behavior of the prepared ceria abrasives with trace metals was evaluated as shown in Figure S2. The observed zeta potential was lower than -30 mV for both of the trace metals used in this experiment. This indicates that there is no agglomeration of ceria abrasives; however, the SEM (Figure S3) results suggest that agglomeration exists. Hence, there might exist complex chemical bonding between the trace metals and the ceria abrasive.

After evaluation of the ceria abrasive stability with different concentrations of trace metals, the same prepared ceria abrasive was utilized for the CMP process of the SiO<sub>2</sub> wafers. The measured MRR is shown in Figure 2. For the ceria abrasive without trace metals, the MRR was found to be 5123.86 Å/min. In the case of ceria abrasive with FeCl<sub>2</sub>, the maximum MRR was observed for 10 ppm FeCl<sub>2</sub> and was 5621.21 Å/min, while for the ceria abrasive with CrCl<sub>2</sub>, the maximum MRR was observed for 50 ppm CrCl<sub>2</sub> and was 6522.91 Å/min.

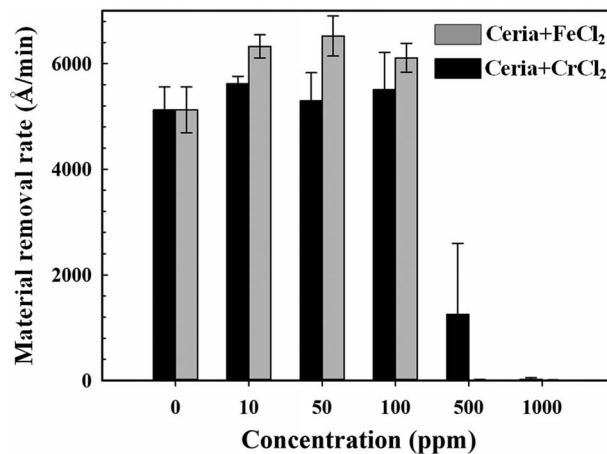


**Figure 2.** Material removal rate of the SiO<sub>2</sub> film for different concentrations of FeCl<sub>2</sub> and CrCl<sub>2</sub>.

This indicates that the ceria abrasive reacted more strongly with CrCl<sub>2</sub> than FeCl<sub>2</sub> and that trace metals help to improve the adhesion between the ceria abrasive and SiO<sub>2</sub> wafer. It has been previously reported that the performance of ceria abrasive mainly relies on the chemical activity of the abrasive surface.<sup>14</sup> The main chemical reaction between the ceria abrasive and SiO<sub>2</sub> relies on the existence of +3 state cerium ions on the ceria surface.<sup>15</sup> The Ce<sup>3+</sup> on the ceria surface can be explained using a simple defect model.

A simple defect model may be constructed by analogy with the Kroger-Vink notation.<sup>16</sup> In other words, Ce<sup>4+</sup> changes to Ce<sup>3+</sup> on the ceria abrasive surface due to the redox reaction process and CrCl<sub>2</sub> more easily changes due to the spontaneous reaction with Ce. This means that the Ce-O-Si structures after adding 50 ppm CrCl<sub>2</sub> are much stronger than the structures before adding CrCl<sub>2</sub> during polishing.<sup>17</sup> This indicates that the redox reaction of ceria abrasive can occur using trace metals.

Because the standard electrode potential of Cr<sup>2+</sup>/Ce<sup>4+</sup> pair ( $E^0 = 2.18$  V/SHE) is much higher than that of Fe<sup>2+</sup>/Ce<sup>4+</sup> pair ( $E^0 = 0.67$  V/SHE), ceria abrasive could be quickly deoxidized by Cr<sup>2+</sup> at room temperature.<sup>18</sup> In solution, the above reaction occurs at the interface between aqueous solution of CrCl<sub>2</sub> and ceria abrasive. As a result, oxygen vacancies can be formed for the process. Upon the formation of neutral oxygen vacancies in the surface of the ceria support, two electrons still remain in each oxygen atom. Using Korger-Vink notation,<sup>19</sup> the two electrons from the oxygen atom are transferred to two different cerium ions neighboring the vacancy site, reducing these cerium ions from the +4 state to the +3 state. After the formation of vacancies on the ceria surface via interaction with the trace metals, Ce<sup>3+</sup> reactive sites are formed.

Further, to better understand the ceria surface, absorption spectroscopy was carried out for the ceria abrasive with different concentrations of trace metals. The absorption spectra for the range of 250 to 400 nm are shown in Figures 3a, 3b. The absorption peak is 295 nm, which agrees with the absorption of Ce<sup>3+</sup> ions.<sup>20-23</sup> The absorption at 295 nm is clearly visible up to 100 ppm CrCl<sub>2</sub>; however, for 500 and 1000 ppm, there was no absorption. Similarly, there is no absorption peak for 1000 ppm FeCl<sub>2</sub>. This strongly supports the sedimentation of ceria abrasive as observed in Figure S1. The absorption at 295 nm for ceria abrasive with FeCl<sub>2</sub> and CrCl<sub>2</sub> is plotted in Figures 3c, 3d. In both samples, the absorption peak is at its maximum for the 50 ppm concentrations of the trace metals. These observations are in close agreement with the MRR results depicted in Figure 2.

It is well known that in the case of a high MRR, there are more opportunities for sub-micron scratches to develop on the SiO<sub>2</sub> wafer. Hence, the surface properties (such as sub-micro scratch) of the SiO<sub>2</sub> wafer after CMP were evaluated via AFM, as shown in Figures. 4a-4c. The RMS roughness for ceria abrasive without trace metals was

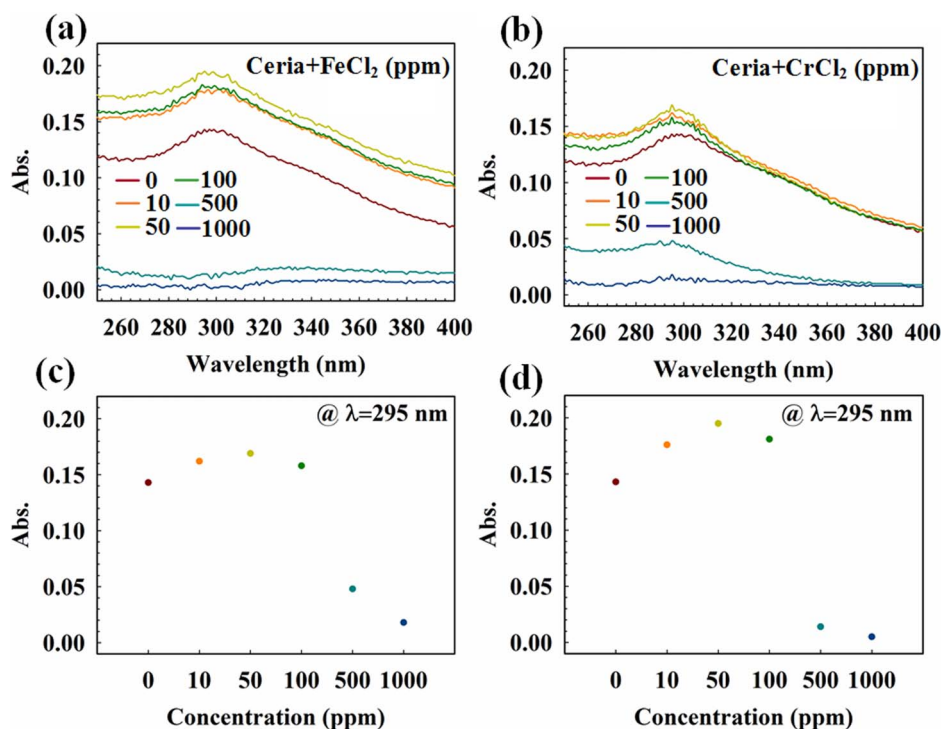


**Figure 3.** UV-vis spectroscopy data for ceria abrasive in the presence of (a)  $\text{FeCl}_2$  and (b)  $\text{CrCl}_2$ . The absorbance peak is at 295 nm with a pH 10.

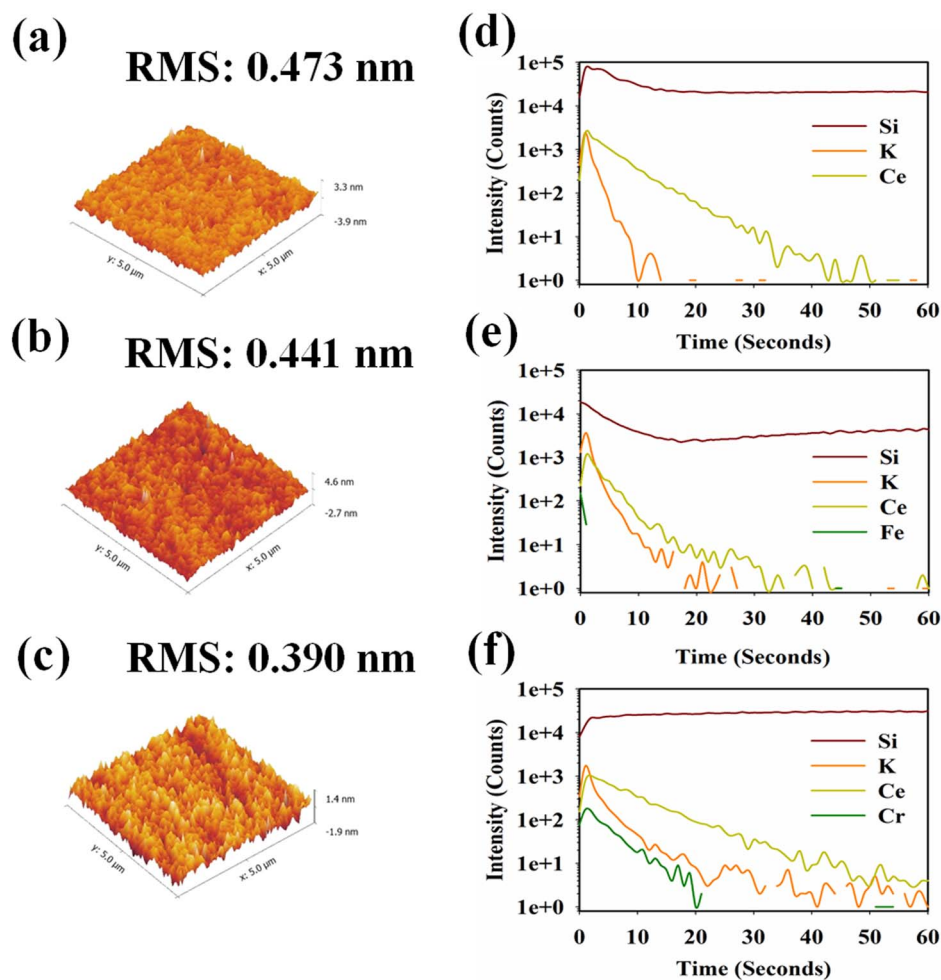


**Figure 4.** AFM images of the  $\text{SiO}_2$  film: (a) after polishing with ceria abrasive without trace metals, and after polishing with the presence of (b)  $\text{FeCl}_2$  and (c)  $\text{CrCl}_2$  at concentrations of 100 ppm. SIMS depth profile spectra of the  $\text{SiO}_2$  film after polishing with (d) ceria abrasive, (e)  $\text{FeCl}_2$ , and (f)  $\text{CrCl}_2$ .



found to be 0.473 nm. However, for 10 ppm  $\text{FeCl}_2$  and 50 ppm  $\text{CrCl}_2$ , the RMS roughness was 0.441 and 0.390 nm, respectively, without any sub-micron scratches on the  $\text{SiO}_2$  wafer. The results for the other concentrations are shown in Figure S4. Further, the defects and diffusion resulting from the trace metals during CMP were measured via SIMS, and these observations are depicted in Figures 4d–4f. It was confirmed that Ce and K exist on the  $\text{SiO}_2$  wafer surface alongside the trace metal ions. For the ceria abrasive with  $\text{FeCl}_2$ , there was no noticeable change in Ce permeation, whereas Ce was deeply permeated for the ceria abrasive with  $\text{CrCl}_2$ . This implies that ceria abrasive with  $\text{CrCl}_2$  is more reactive with the  $\text{SiO}_2$  wafer surface. Generally, post CMP cleaning is carried out to remove any defects, such as ceria abrasive residues on the  $\text{SiO}_2$  wafer.<sup>24,25</sup> It may be the case that the minor diffusion caused by ceria abrasive with  $\text{FeCl}_2$  or  $\text{CrCl}_2$  can mitigated during the etching process of post CMP cleaning. Hence, minor diffusion of the trace metals along with Ce may not be considered as a critical issue during the CMP process.

### Summary

In summary, the effectiveness of the two trace metals  $\text{FeCl}_2$  and  $\text{CrCl}_2$  was successfully evaluated for an improved MRR in the CMP process. The observed zeta potential was less than  $-30$  mV for both trace metals, indicating that there is no agglomeration of ceria abrasives. However, the SEM results show agglomeration, which might be due to the existence of complex chemical bonding between the trace metals and ceria abrasive. Significant enhancement of the MRR was observed for  $\text{CrCl}_2$  at 50 ppm, indicating that the presence of  $\text{CrCl}_2$  improves the adhesion between the ceria abrasive and  $\text{SiO}_2$  wafer. The results of this study will provide researchers and engineers apply trace metals in ceria abrasives to improve the CMP process, regardless of minor trace metals diffusion possibilities.

### Acknowledgments

This work was supported by the National Research Foundation of Korea (NRF) grant funded by the Korea government (MEST) (NRF-2017R1A2B3011222).

### References

1. J. Seo, J. Moon, Y. Kim, K. Kim, K. Lee, Y. Cho, D.-H. Lee, and U. Paik, *ECS Journal of Solid State Science and Technology*, **6**(1), P42 (2017).
2. C. Yan, Y. Liu, J. Zhang, C. Wang, W. Zhang, P. He, and G. Pan, *ECS Journal of Solid State Science and Technology*, **6**(1), P1 (2017).
3. J. C. Yang, D. W. Oh, H. J. Kim, and T. Kim, *Journal of electronic materials*, **39**(3), 338 (2010).
4. R. K. Singh, S.-M. Lee, K.-S. Choi, G. B. Basim, W. Choi, Z. Chen, and B. M. Moudgil, *MRS bulletin*, **27**(10), 752 (2002).
5. C. Shin, H. Qin, S. Hong, S. Jeon, A. Kulkarni, and T. Kim, *Journal of Mechanical Science and Technology*, **30**(12), 5659 (2016).
6. J. C. Yang, D. W. Oh, G. W. Lee, C. L. Song, and T. Kim, *Wear*, **268**(3), 505 (2010).
7. Y. G. Wang, L. C. Zhang, and A. Biddut, *Wear*, **270**(3), 312 (2011).
8. L. Wang, K. Zhang, Z. Song, and S. Feng, *Applied surface science*, **253**(11), 4951 (2007).
9. Y. Lee, Y.-J. Seo, H. Lee, and H. Jeong, *International Journal of Precision Engineering and Manufacturing-Green Technology*, **3**(1), 13 (2016).
10. H.-G. Kang, T. Katoh, M.-Y. Lee, H.-S. Park, U. Paik, and J.-G. Park, *Japanese journal of applied physics*, **43**(8B), L1060 (2004).
11. Y. Chen, J. Lu, and Z. Chen, *Microelectronic Engineering*, **88**(2), 200 (2011).
12. R. Manivannan and S. Ramanathan, *Microelectronic Engineering*, **85**(8), 1748 (2008).
13. S. Jang, A. Kulkarni, H. Qin, and T. Kim, *Review of Scientific Instruments*, **87**(4), 046101 (2016).
14. T. Hoshino, Y. Kurata, Y. Terasaki, and K. Susa, *Journal of Non-Crystalline Solids*, **283**(1), 129 (2001).
15. E. Tolstobrov, V. Tolstoi, and I. Murin, *Inorganic materials*, **36**(9), 904 (2000).
16. M. Mogensen, N. M. Sammes, and G. A. Tompsett, *Solid State Ionics*, **129**(1), 63 (2000).
17. J. Paier, C. Penschke, and J. Sauer, *Chemical reviews*, **113**(6), 3949 (2013).
18. Z. Wang, D. Luan, S. Madhavi, C. M. Li, and X. W. D. Lou, *Chemical Communications*, **47**(28), 8061 (2011).
19. F. Kröger and H. Vink, *Journal of Physics and Chemistry of Solids*, **5**(3), 208 (1958).
20. P. V. Dandu, B. Peethala, and S. Babu, *Journal of The Electrochemical Society*, **157**(9), H869 (2010).
21. P. V. Dandu, V. Devarapalli, and S. Babu, *Journal of colloid and interface science*, **347**(2), 267 (2010).
22. P. V. Dandu, B. Peethala, H. Amanapu, and S. Babu, *Journal of The Electrochemical Society*, **158**(8), H763 (2011).
23. S. Babu and V. P. Dandu, in "Optical Fabrication and Testing", p. OM2D. 1. Optical Society of America, 2012.
24. Y.-H. Kim, S.-K. Kim, J.-G. Park, and U. Paik, *Journal of The Electrochemical Society*, **157**(1), H72 (2010).
25. D. Volkov, P. V. Dandu, H. Goodman, B. Santora, and I. Sokolov, *Applied Surface Science*, **257**(20), 8518 (2011).